

Phase Error Correction for Synthetic-Aperture Phased-Array Imaging Systems

J.R. Fienup*

Advanced Information Systems Group
Veridian ERIM International
P.O. Box 134008
Ann Arbor, MI 48113-4008

ABSTRACT:

If one replaces the ordinary single receiver of a synthetic-aperture radar (SAR) with a linear array of receivers underneath the wings of an aircraft, one obtains a 3-D signal history (two spatial dimensions plus the frequency dimension) that allows the computation of a 3-D image (angle-angle-range) of a scene. Because of the limited extent of the wingspan, the cross-track resolution is limited, driving one to use high frequencies, such as 94 GHz, having a wavelength of 3.2 mm. At such short wavelengths, the motion of the wings during the synthetic-aperture integration time will cause large phase errors that will severely blur the image. This paper describes an approach to measuring and correcting these and other phase errors. The approach involves having three transmitters, each at a slightly different monotone frequency. Relative to the first receiver, the second is displaced along the direction of the array of receivers and the third is displaced perpendicular to that direction. The array of receivers can separate the three corresponding signals reflected from the ground from one another. We will show mathematical analysis that allows us to determine the phase errors at each receiver from these three signals. It is required either that the three transmitters experience the same phase errors (so they should be rigidly mounted together) or that the phase errors at the three transmitters are measured. No measurement of phase errors on the receivers is required.

Keywords: Synthetic-aperture radar, SAR, synthetic aperture, 3-D imaging, motion compensation, phase errors

1. BACKGROUND

Among the proposed capabilities of the DARPA-funded MM-Wave Targeting and Imaging Sensor (MWTIS) program is a downward-looking 3-D SAR sensor, as illustrated in Figure 1.

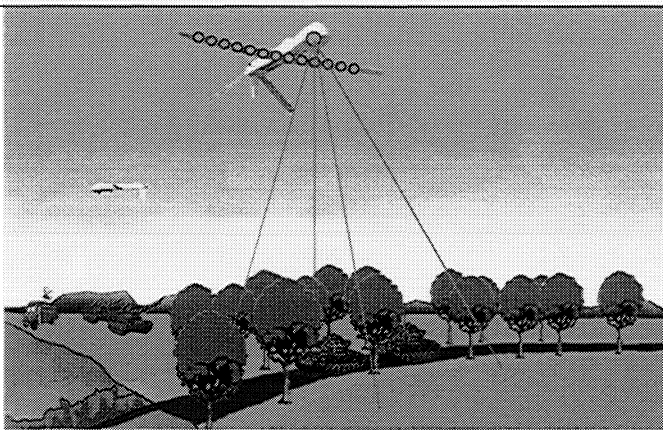


Figure 1. 3-D Sensor Concept.

A 1-D array of receivers under the wing sweeps out a 2-D aperture with time, and the third dimension is achieved by ranging.

*Correspondence: Email: fienup@erim-int.com; Telephone: 734 994-1200 ext. 2500

It obtains fine resolution in the height dimension by ranging, in the along-track dimension by a synthetic aperture, and in the cross-track dimension by a real array of receivers on the underside of the wing of an airborne sensor. That is, in the height and along-track dimension it is acting as a SAR, conventional except for the direction in which it is pointed, and as a phased array (upon receive) antenna in the cross-track direction. A similar system was built and flown over 25 years ago.¹ It would operate at W-band (94 GHz, with a wavelength of 3.2 mm) which allows good resolution at a 15,000-ft altitude (above the clouds) using the wing span of the Predator™ unmanned aerial vehicle (UAV). It can alternatively operate as a down-looking angle-angle imaging system by using a single frequency rather than the wide bandwidth needed for ranging. Details of the sensor are described elsewhere. A challenging aspect of the down-looking 3-D SAR is its motion compensation requirements. This paper describes a novel system that promises to solve this unique and difficult motion compensation problem. It uses of a set of three transmitters, each operating at a slightly different narrow-band frequency outside the frequency band used for imaging. The three sets of signals, one from each of the transmitters, reflected from the ground below and measured by array of receivers, gives sufficiently redundant measurements to separate the phase due to unknown motion from the phase due to the reflectivity of the ground. The phase error determined from these measurements can then be subtracted from the phase of the imaging waveform to correct it and form a focused image despite the deleterious motions.

2. MOTION COMPENSATION REQUIREMENTS

Unknown radial motions of an active sensor antenna, relative to the scene by a distance Δr , cause phase errors of $\phi_e = 2\pi\Delta r/\lambda$ for wavelength λ . If the transmitter and receiver both experience the same Δr , then the total phase error is $4\pi\Delta r/\lambda$. For diffraction-limited, good-quality imagery without noticeable smearing, we need Δr (peak-to-valley) $< \lambda/4$, or $\Delta r_{\text{rms}} < \lambda/14$. For $\lambda = 3.2$ mm, this means that the motion must be measured and compensated to sub-mm accuracies. In contrast to this, the wing tips of the Predator UAV can “flap” with motions up to 300 mm, two orders of magnitude greater than this. From this we see that the motion compensation problem is severe for a down-looking sensor on the Predator. If linear phase errors only translate the image, so we will ignore them.

To achieve an along-track resolution of 1 m, comparable to that of the cross-track resolution, we need an integration time of $T_{\text{sub}} = (7 \text{ m}/2) / 40\text{m/sec} = 0.09$ sec for one sub-image. Several sub-images could be mosaicked together to form a larger image. Table 1 defines the symbols used in this paper and lists example values for example calculations.

Table 1. System Parameters

Symbol	Description	Nominal Value
f_c	center frequency	94 GHz
λ	wavelength	3.2 mm
v_p	platform forward velocity	40 m/sec
c	speed of light	3×10^8 m/sec
h	altitude of platform	4,572m (15,000 ft)
Δr	radial deviation of antenna position	various
ϕ	phase error	various
T	integration time for entire image	various
T_{sub}	integration time for sub-image	0.9 to 3 sec
D_{act}	cross-track array width	7 m
θ_{ct}	cross-track IFOV	$\pm 10^\circ$
θ_{at}	along-track IFOV	$\pm 5^\circ$
m, n	aperture coordinates: pulse number and wing position	various

3. MOTION COMPENSATION APPROACH

The undesirable motion can be measured and compensated in a number of different ways. The combination of global positioning sensors (GPSs) and inertial measurement units (IMUs) to form an inertial navigation sensor (INS) can often provide most of the necessary motion compensation for a conventional SAR. For the 3-D down-looking SAR, however, we could have hundreds of receivers, each with a different motion, so the conventional combination of INS plus SAR motion compensation will be too complicated and expensive. We assume that there will, however, be an INS at the transmitter, since there is only one of them. Another possibility is to use strain gauges within the wings of the platform to measure the motion of the wing. It has not been demonstrated that this will be adequate for measuring Δr to within a fraction of a millimeter under realistic flight conditions. For these reasons we need another motion measurement approach.

For determining the motion of the array of receiver antennas, we invented an approach using three transmitters and the array of receivers. Figure 2 depicts the receiver array across the wing and potential locations of the three transmitters. One of the three transmitters could be the transmitter used for the 3-D SAR imaging. However, it is easier to consider three separate transmitters that are used only for the motion sensing approach.

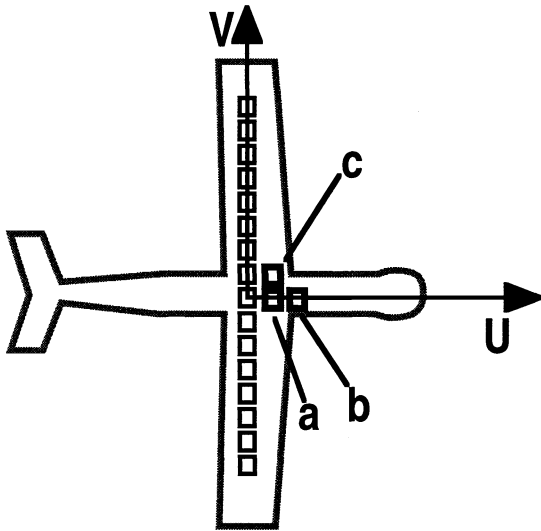


Figure 2. Sensor/Platform Configuration
Three transmitters (*a*, *b*, *c*) and a row of receivers along wings.

Suppose that at time $t = 0$ we transmit a pulse (of duration some fraction of a millisecond) at a constant frequency ω_a from antenna *a* and receive at locations $(u, v) = (0, n\Delta v)$ along the wing of the platform, as illustrated in Figure 2. At times $t = m\tau$, $m = 1, \dots, M - 1$, we repeat the measurements, thereby sweeping out the 2-D field reflected by the scene below. If we make adequately sampled heterodyne measurements and there were no phase errors, then we could Fourier transform the received field data to compute a coherent 2-D angle-angle image of the scene (two of the three dimensions of the 3-D down-looking SAR system). In practice, however, there will be phase errors due to unknown motion. For the m^{th} pulse, let the phase error on the transmitter be ϕ_{am} and the phase error on the n^{th} receiver be ϕ_{mn} . The field measurements originating from antenna *a* would then be

$$G_{amn} = F_{mn} \exp[i(\phi_{mn} + \phi_{am})] , \quad (1)$$

where F_{mn} are the ideal complex field measurements without phase errors (ignoring noise). Note that the phase error ϕ_{mn} is fully two-dimensional and is not separable. We wish to determine and correct the total phase errors $(\phi_{mn} + \phi_{am})$, allowing us to obtain an unblurred image.

Now suppose, as shown in Figure 2, we simultaneously illuminate with antennas b and c , which have phase errors ϕ_{bm} and ϕ_{cm} , respectively, and frequencies ω_b and ω_c , respectively. The difference in frequencies is chosen to be large enough to allow us to electronically separate the three fields at the receiver. For simplicity, choose the position of antenna b to be $v_p \tau/2$ ahead of antenna a , where v_p is the forward velocity of the platform; this shifts the field one sample ahead. Also for simplicity, choose antenna c to be separated from antenna a by a distance equal to the separation between the receivers on the wing. Then the field measurements that originate from the second (b) antenna will be

$$G_{bmn} = F_{m+1,n} \exp[i(\phi_{mn} + \phi_{bm})] . \quad (2)$$

That is, the field F will shift one sample over the receivers, but the phase errors are the same (for the same received pulse, the m^{th} pulse). Similarly, the field measurements that originate from the third (c) antenna will be

$$G_{cmn} = F_{m,n+1} \exp[i(\phi_{mn} + \phi_{cm})] , \quad (3)$$

where again the field shifts (along the wing in this case) but the phase errors do not. We notice that

$$G_{amn} G_{bmn}^* = |F_{mn}|^2 \exp[i(\phi_{mn} - \phi_{m-1,n} + \phi_{am} - \phi_{bm-1})] . \quad (4)$$

This sheared product, computed from measured quantities, contains information about how the phase error varies with time (m). The phase of the field itself, F_{mn} , is canceled. Similarly,

$$G_{amn} G_{cmn}^* = |F_{mn}|^2 \exp[i(\phi_{mn} - \phi_{m,n-1} + \phi_{am} - \phi_{cm})] . \quad (5)$$

This second sheared product contains information about how the receiver phase error varies along the wing (n).

One way to proceed from here would be to put inertial measurement units (IMU's) on the three transmitters, thereby measuring ϕ_{am} , ϕ_{bm} , and ϕ_{cm} . Then using the products above, after subtracting the phase error due to the transmitters, we have the finite differences of the phase error ϕ_{mn} in the two directions, for which there exist well-developed complex-phaser reconstruction algorithms to determine ϕ_{mn} .² The complex-phaser reconstructor solves over the entire array in a least-squares fashion and takes care of problems with phase branch cuts. This approach was inspired by an approach to image reconstruction through atmospheric turbulence,³ but here we reverse the roles of the phase due to the object reflectivity and the phase due to the aberrations.

An alternative to having three IMU's (one for each transmitter) is, since the three transmitters are physically close to one another, to rigidly mount them all together, so that they all experience the same phase error: $\phi_{am} = \phi_{bm} = \phi_{cm}$. This would be true if the only significant source of the phase error on the transmitters was changes in altitude. This would not be true, however, for roll or for pitch. However, if the common IMU were to accurately measure roll and pitch, then that effect could be backed out.

When $\phi_{am} = \phi_{bm} = \phi_{cm}$, (or we can measure the phase errors of the transmitters and compensate for them), then from the equations above we see that the phase of the second product, $G_{amn} G_{cmn}^*$, is $\phi_{mn} - \phi_{m,n+1}$, where the phase error due to receivers a and c have canceled. This gives us information about the phase error in the direction of the wing. However, from the first product, the phases $\phi_{am} - \phi_{bm-1} \approx \phi_{am} - \phi_{am-1}$ from transmitters a and b do not cancel. Nevertheless, the phase of $G_{amn} G_{bmn}^*$, namely

$$\arg[G_{amn}G_{bm-1,n}^*] = \phi_{mn} - \phi_{m-1,n} + \phi_{am} - \phi_{am-1} = (\phi_{mn} + \phi_{am}) - (\phi_{m-1,n} - \phi_{am-1}), \quad (6)$$

is just the finite difference in the total phase error ($\phi_{mn} + \phi_{am}$) from both the receiver and the transmitter (modulo 2π). We can think of the product $G_{amn}G_{cm,n-1}^*$ as being an orthogonal shear of the same total phase error, except that its shear happens to cancel the ϕ_{am} term, and so that term does not appear explicitly in the equation for $G_{amn}G_{cm,n-1}^*$. Hence, when we use $G_{amn}G_{bm-1,n}^*$ and $G_{amn}G_{cm,n-1}^*$ in the phasor reconstructor, the output is an estimate of the total phase error ($\phi_{mn} + \phi_{am}$). Thus, in the absence of noise and with $\phi_{am} = \phi_{bm} = \phi_{cm}$, we should expect a perfect reconstruction of the phase.

For the case of an unknown pitch, $\phi_{am} = \phi_{cm} \neq \phi_{bm}$, and we would expect to have a residual phase error in the along-track direction. We could perform an initial phase estimate, using the phasor reconstructor, assuming $\phi_{am} - \phi_{bm-1} = 0$, and the residual error in the resulting reconstruction appears to be a function of m only. Then to account for the fact that $\phi_{am} - \phi_{bm-1} \neq 0$, we would refine the phase estimate; for this we can use conventional SAR focusing algorithms, which work well on 1-D phase errors.

For the case of roll and pitch, $\phi_{am} \neq \phi_{cm} \neq \phi_{bm}$, and a 2-D residual phase error would result from the phasor reconstructor. For this kind of phase error, conventional SAR autofocus approaches do not work, and the phase correction becomes problematical.

4. SOURCES OF RESIDUAL PHASE ERRORS

The three-antenna motion measurement approach can have residual phase errors due to several effects. In this paper we show the effects of (i) noise, (ii) unknown differences in phase errors amongst the three transmitters due to platform roll and pitch changes, and (iii) errors in knowledge of forward velocity.

To test the effect of noise on the phase-error estimate, we performed a digital simulation of the sensed signals and exercised the reconstruction algorithms on them. We simulated a phase error consisting of the sum of (i) a 2-D phase error consisting of a quadratic phase error along the wing direction, the coefficient of which varied with time, corresponding to wings flapping up and down, and (ii) a 1-D phase error function of time only, corresponding to platform altitude changes. We assumed that all three transmitters and all the receivers suffered from the same 1-D phase error. Figure 3 shows the total 2-D phase error at the receiver and a cut through it at the position of the center of the fuselage. Note that 40 radians corresponds to over six wavelengths and 20 mm of wing motion, which can easily happen.

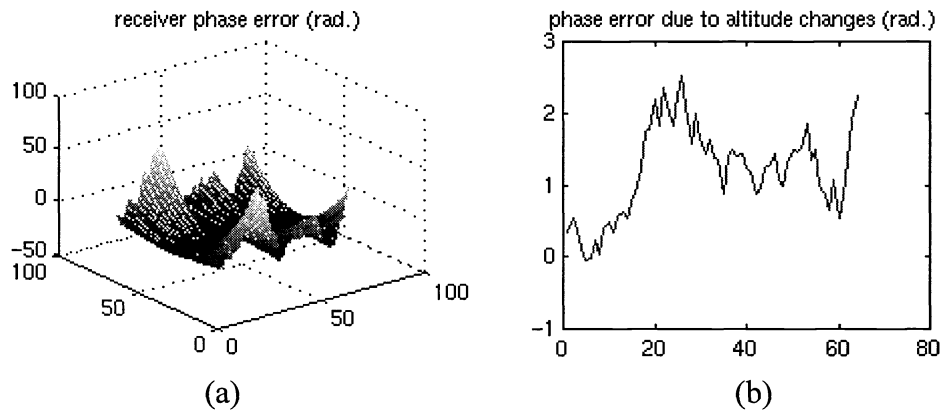


Figure 3. Simulated Phase Error. (a) 2-D phase error, (b) 1-D altitude component of phase error.

We simulated a coherent scene by (1) adding together two displaced computer-generated images, one of a T72 tank and the other of an SRT; (2) adding a uniform random clutter background in the pixels outside the bright areas of the targets; and (3) low-pass filtering by truncating the Fourier transform, thereby simulating the effects of a finite aperture.

Figure 4 shows the simulated image of the scene and the image degraded by the phase error. The phase error is severe enough that the degraded image is completely unrecognizable. From the Fourier transforms of the degraded image and two more like it simulated from the other two transmit antennas (with appropriate translations of the signals from the scene relative to the phase errors), we computed the two sheared products described above and fed them into a phasor reconstructor. The output phase-error estimate was used to correct the data to give the corrected image, shown in the bottom left of the figure. For the case of no noise, the reconstruction was perfect. We added independent circular-complex Gaussian random noise to the three received signals and ran the reconstruction algorithm on the noisy data. An example for an amplitude signal-to-noise ratio (SNR) of 8 is shown in Figure 4. The residual phase error is shown in the lower right. We reran the simulation and reconstruction algorithms for several noise realizations. The results are plotted in Figure 5. We see that to have high probability of the residual error from the three-transmitter system being acceptably low (rms phase error less than 1/14 wave), we need a SNR of about 10 or 15. This results in images that are visually nearly indistinguishable from the ideal image.

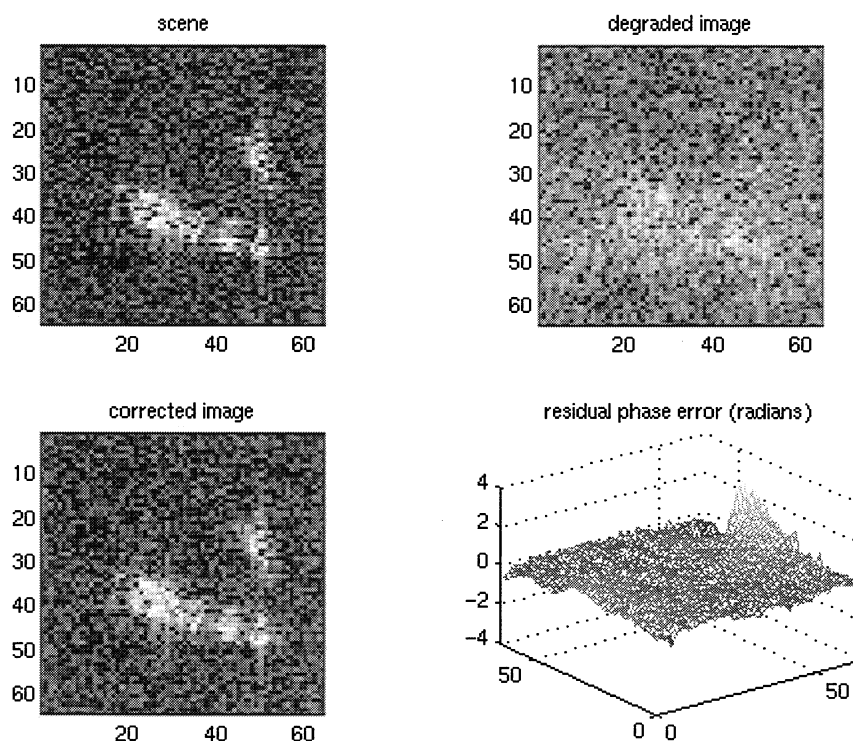


Figure 4. Reconstruction Results, SNR = 8 Original scene, blurred image of scene, corrected image, and residual phase error. The residual rms phase error is 0.41 rad. (1/15.4 wave).

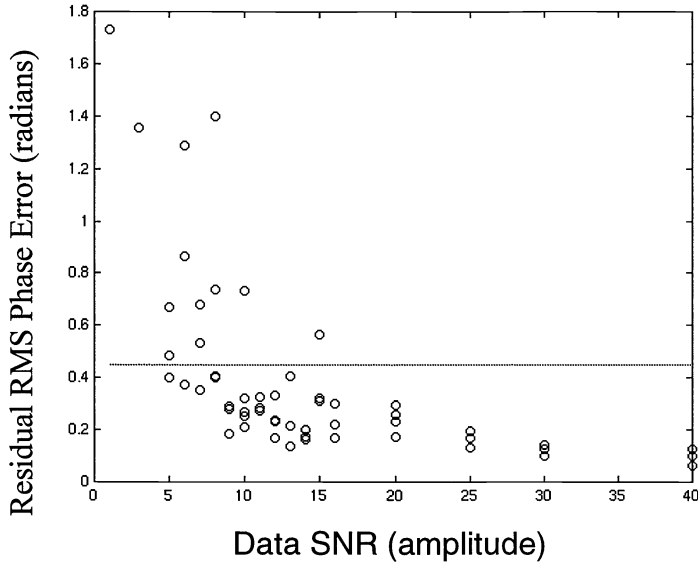


Figure 5. Residual Phase Error versus SNR. For excellent quality imagery (rms phase error < 1/14 wave, indicated by the solid line), need data SNR > 10 or 15.

If the platform experiences pitch or roll, then the three transmitters experience slightly different phase errors. If the pitch or roll is an unknown constant angle during T_{sub} , then it causes a linear phase error and a translation of the sub-image with no blurring. Unknown pitch or roll that varies with time over the interval T_{sub} will cause a blurring of the image.

For the case of pitch, $\phi_{\text{am}} \neq \phi_{\text{bm}}$. If the instantaneous pitch angle is θ_{pm} , then the first sheared product becomes

$$G_{\text{amn}}G_{\text{bm-1,n}}^* = |F_{\text{mn}}|^2 \exp\{i[\phi_{\text{mn}} - \phi_{\text{m-1,n}} + \phi_{\text{am}} - \phi_{\text{am-1}} + 2\pi\Delta u \theta_{\text{pm}}/\lambda]\} . \quad (7)$$

This differs from the ideal sheared product in that it has the additional phase term $2\pi\Delta u \theta_{\text{pm}}/\lambda$. In one dimension the effect of the phasor reconstructor is to perform a cumulative summation. For the case of a pitch that increases linearly to pitch θ_{pT} during the aperture time, the error in the phase estimate can be shown to be quadratic, with a center-to-edge value of $\phi_{\text{eM}} = (M + 1)(\pi\Delta u \theta_{\text{pT}}/4\lambda)$. For example, for $M = 200$ samples, $\Delta u = 7$ cm, $\lambda = 3.2$ mm, to keep the error down to, say one 1/4 wave, we would need to have the unknown change in pitch be less than 0.027° during the aperture time. Figure 6 shows the effect on the motion compensation approach of an unknown pitch change of 0.2° during the aperture time. It confirms the analysis predicting a quadratic phase error. The residual quadratic phase error for such a case cause significant blurring.

In general, if the pitch varies in time as an n^{th} -order polynomial, then the error in the phase estimate will be an $(n+1)^{\text{st}}$ -order polynomial in time.

Recall that an unknown linearly varying pitch of 0.027° during the aperture time results in a phase error of 1/4 wave (peak-to-valley). The most obvious way to meet this requirement is to have an INS measure the pitch of the platform at the receivers. Since INSs are reported to be able to measure angles as small as 0.0006° , this appears to be very reasonable. Another alternative would be to employ a standard SAR autofocus algorithm to correct the residual error due to changing pitch — this is possible because changes in pitch cause a one-dimensional phase error (in the along-track dimension), which is what SAR autofocus algorithms are designed to handle.

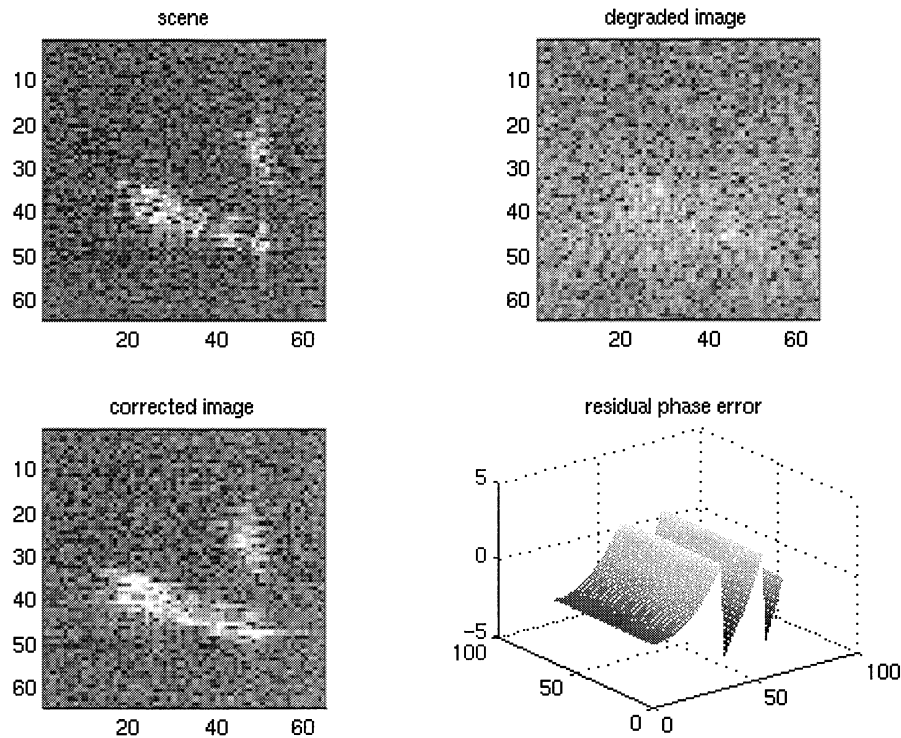


Figure 6. Reconstruction Results with Unknown Pitch of 0.2. Original scene, blurred image of scene, corrected image, and residual phase error (wrapped modulo 2π).

For the case of roll alone, we find a similar sensitivity, but the residual phase errors are two dimensional and non-separable, making them less amenable to correction by conventional SAR autofocus algorithms. Hence we would rely on the INS at the transmitters to measure the roll to an accuracy of 0.027° , which can be readily accomplished.

If there is an error in the forward velocity of the platform, then for the three-transmitter approach to motion compensation, the fields in the sheared products would not line up properly, and the phases of the fields reflected from the scene would not cancel. The fields must be registered by a fraction of a Nyquist sample. Figure 7 plots the residual phase error as a function of forward velocity error for a set of computer simulations. It shows that the forward velocity error must be below 10 to 12% (fraction of a pixel misregistration) to achieve an acceptably low residual phase error.

5. SUMMARY

We developed a method for sensing the phase errors along a phased-array, synthetic-aperture receiver using three transmitters, and analyzed the potential for residual phase errors. The following requirements on the system retain the residual errors at an acceptable level:

- Received signal-to-noise ratio better than 10 or 15.
- Inertial navigation system (INS) at the transmitters that measures roll and pitch to better than 0.027 degrees during the integration time for a sub-image (0.9 sec to 3 sec, depending on along-track resolution).
- INS that measures forward velocity to within 10%.

We also found that the three distinct frequencies for the three transmitters must differ from one another by at least 30 kHz, but span no more than 1 MHz, and are outside the band used for imaging.

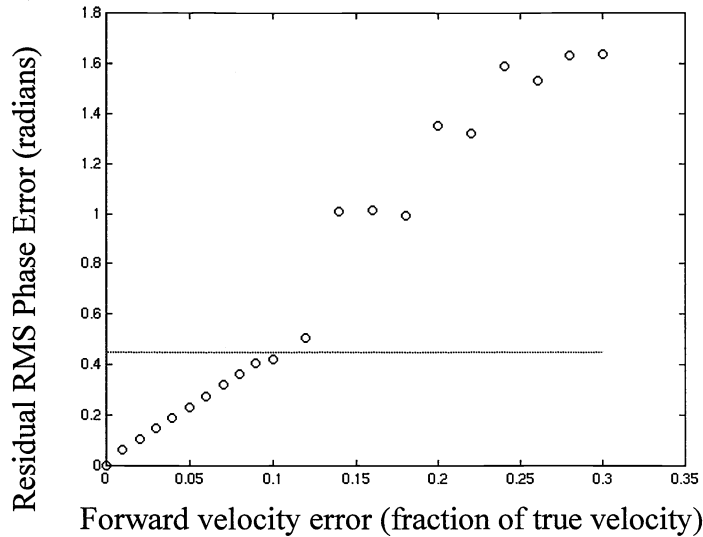


Figure 7. Residual Phase Error Due to Forward Velocity Error. For excellent quality imagery (rms phase error $< 1/14$ wave, indicated by the solid line), need forward velocity error < 0.12 pixels.

All of these requirements appear to be easy to meet, making the motion compensation system appear to be practical to implement.

ACKNOWLEDGEMENTS

The author thanks Brad Tousley for providing a graphic which was modified to make Figure 1. This material is based upon work supported by subcontract H818901 which was awarded under prime contract DAAL01-98-C-0068 awarded to General Atomics by the Army Research Laboratory (ARL) with sponsorship by the Defense Advanced Research Projects Agency (DARPA). Any opinions, findings and conclusions or recommendations expressed in this material are those of the author and do not necessarily reflect the views of the US Army. The U.S. Government is authorized to reproduce and distribute reprints for Government purposes notwithstanding any copyright notation hereon.

REFERENCES

1. Larson, R.W., et al., "A Microwave Hologram Radar System," IEEE Transactions on Aerospace and Electronic Engineering, AES-8(2), March 1972.
2. See, for example, P. Nisenson, "Speckle Imaging with the PAPA Detector and the Knox-Thompson Algorithm," in D.M. Alloin and J.-M. Mariotti, eds., Diffraction-Limited Imaging, 13- 23 Sept. 1988 (Kluwer Academic Publishers, Boston, 1989), pp. 157-169.
3. R.A. Hutchin, "Sheared Coherent Interferometric Photography: A Technique for Lensless Imaging," in digital Image Recovery and Synthesis II, Proc. SPIE 2029, 161-168 (1993).